

Ultraviolet B but not Ultraviolet A Radiation Initiates Melanoma

Edward C. De Fabo,¹ Frances P. Noonan,¹ Thomas Fears,² and Glenn Merlino³

¹Laboratory of Photobiology and Photoimmunology, Department of Environmental and Occupational Health, School of Public Health and Health Services, The George Washington University Medical Center, Washington, DC; ²BioStatistics Branch, National Cancer Institute, Bethesda, Maryland; and ³Molecular Genetics Section, Laboratory of Molecular Biology, National Cancer Institute, Bethesda, Maryland

Abstract

Cutaneous malignant melanoma is one of the fastest increasing cancers with an incidence that has more than doubled in the last 25 years. Sunlight exposure is strongly implicated in the etiology of cutaneous malignant melanoma and the UV portion of the sunlight spectrum is considered responsible. Data are, however, conflicting on the roles of ultraviolet B [UVB; 280–320 nanometers (nm)] and ultraviolet A (UVA; 320–400 nm), which differ in their ability to initiate DNA damage, cell signaling pathways and immune alterations. To address this issue, we have used specialized optical sources, emitting isolated or combined UVB or UVA wavebands or solar simulating radiation, together with our hepatocyte growth factor/scatter factor-transgenic mouse model of UV-induced melanoma that uniquely recapitulates human disease. Only UVB-containing sources initiated melanoma. These were the isolated UVB waveband (>96% 280–320 nm), the unfiltered F40 sunlamp (250–800 nm) and the solar simulator (290–800 nm). Kaplan-Meier survival analysis indicated that the isolated UVB waveband was more effective in initiating melanoma than either the F40 sunlamp or the solar simulator (modified log rank $P < 0.02$). The latter two sources showed similar melanoma effectiveness ($P = 0.38$). In contrast, transgenic mice irradiated with either the isolated UVA waveband (>99.9% 320–400 nm, 150 kJ/m²), or an F40 sunlamp filtered to remove > 96% of the UVB, responded like unirradiated control animals. We conclude that, within the constraints of this animal model, UVB is responsible for the induction of mammalian cutaneous malignant melanoma whereas UVA is ineffective even at doses considered physiologically relevant. This finding may have major implications with respect both to risk assessment from exposure to solar and artificial UVB, and to development of effective protection strategies against melanoma induction by UVB. Moreover, these differences in wavelength effectiveness can now be exploited to identify UV pathways relevant to melanomagenesis.

Introduction

Solar radiation reaching the Earth's surface is a continuum of electromagnetic radiation composed, in part, of two ranges of UV wavebands, ultraviolet B (UVB) and ultraviolet A (UVA), and visible light [400–780 nanometers (nm)]. Photobiological processes are wavelength dependent, and these wavebands of radiation have significantly different biological effects (1). The specific waveband(s) responsible for inducing human melanoma are unknown, but the nature of the initiating wavelengths is central to understanding mechanisms of melanomagenesis. Successful prevention strategies for minimizing

exposure to harmful UV radiation from sunlight and artificial sources and accurate risk assessment also require knowledge of the melanoma-effective wavelengths. Because observational epidemiologic studies cannot derive wavelength-dependent information, direct experimentation in a relevant animal model is necessary. The lack, however, of an appropriate animal model for UV-induced melanoma, until now, has prevented the experimental identification of the active melanoma wavebands (2, 3). The emergence of the hepatocyte growth factor/scatter factor (HGF/SF) mouse that uniquely develops, in response to neonatal UV exposure, melanocytic neoplasms in stages that are highly reminiscent of human cutaneous malignant melanoma with respect to biological, genetic, and etiologic criteria, has allowed for the first time an assessment of the individual roles of UVA and UVB in mammalian melanomagenesis (4). The requirement for neonatal UV irradiation in this mouse model parallels the critical role for childhood sunlight exposure revealed by epidemiologic studies of human melanoma (5).

Materials and Methods

Neonatal HGF/SF-transgenic mice were irradiated with a specialized optical source which coupled UV interference or cutoff filters to a 2.5 kW xenon lamp (6, 7), to produce either isolated UVB or UVA wavebands or solar simulating radiation containing UVB, UVA, and visible radiation in proportions approximating sunlight. Neonatal transgenic animals were also irradiated with F40 sunlamps, which produce UVB and UVA radiation and visible light.

The spectral outputs of the sources used are given in Fig. 1 and the doses delivered are listed in Table 1. Following treatment, animals were monitored weekly over 14 months for lesion and tumor development and melanomas were histologically verified as described previously (2, 4). Time to development of the first lesion that subsequently became a melanoma was determined for each animal and used in survival analysis (see Results). In agreement with previous studies (2, 4), by far the majority of melanomas produced by irradiation with any of the effective sources had a junctional component with a variety of pathologies that closely resembled the histopathology of human melanoma. No melanomas were observed in wild-type animals either unirradiated or irradiated with any UV source.

Results and Discussion

To deliver comparable doses from the spectrally different sources, it was necessary to take into consideration differences in wavelength effectiveness at initiating melanoma and to calculate, and then deliver, equivalent biologically effective melanomagenic doses. An appropriate experimentally derived wavelength dependence or action spectrum can be used to account for differences in wavelength efficiency. An action spectrum describes the relative efficiencies of radiation of different wavelengths at production of a particular biological effect (6, 8, 9).

Briefly, to calculate biologically effective doses, the spectral output of a given source is multiplied by the relevant action spectrum. The integral of this product is the biologically effective or "weighted" irradiance for that source (E_{eff}) according to the equation $E_{\text{eff}} = \int A(\lambda)E(\lambda)d\lambda$ where $A(\lambda)$ is the action spectrum in relative units, $E(\lambda)$ is spectral irradiance emitted from a given source, and λ is

Received 4/27/04; revised 7/16/04; accepted 7/22/04.

Grant support: The National Cancer Institute of the NIH, USA, including CA92258 and CA53765S (Mouse Models of Cancer Supplement). E. De Fabo and F. Noonan also thank the Elaine H. Snyder Cancer Research Trust (George Washington University) for additional support.

The costs of publication of this article were defrayed in part by the payment of page charges. This article must therefore be hereby marked *advertisement* in accordance with 18 U.S.C. Section 1734 solely to indicate this fact.

Requests for reprints: Edward De Fabo, Laboratory of Photobiology and Photoimmunology, 112 Ross Hall, Department of Environmental and Occupational Health, School of Public Health and Health Services, The George Washington University Medical Center, 2300 I St. NW, Washington, DC 20037. Phone 202-994-3975; E-mail: drmedc@gwumc.edu.

©2004 American Association for Cancer Research.

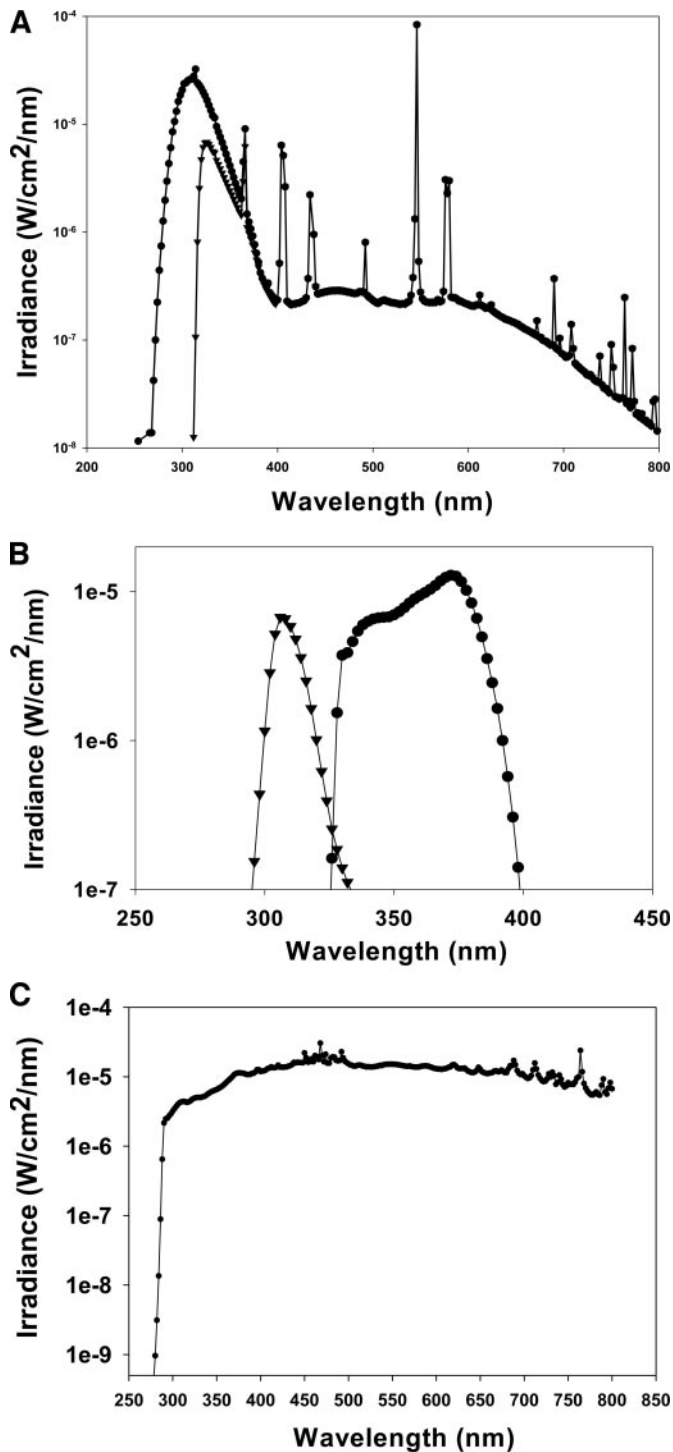


Fig. 1. Spectral output of sources used to irradiate HGF/SF mice. A, a bank of 6 F40 sunlamps either unfiltered (●) or filtered with Mylar (▼) to remove UVB radiation. B, isolated UVB (▼) or UVA (●) wavebands produced using a specialized source that coupled UV interference filters to a 2.5 kW xenon lamp (6). An exposure field (~50 cm²) sufficient for simultaneous irradiation of up to 12 neonatal mice by the selected waveband(s) was produced. C, solar-simulating radiation produced using the 2.5 kW xenon arc source coupled with a 290 nm cutoff filter to deliver solar simulating radiation containing UVB, UVA, and visible radiation approximating sunlight. All radiation measurements were performed using a spectroradiometer (Model 742, Optronic Laboratories, Inc., Orlando, FL).

wavelength. From the biologically effective irradiance, the biologically effective dose (D_{eff}) is calculated as $D_{\text{eff}} = E_{\text{eff}} \times \text{exposure time}$ (10).

No mammalian melanoma action spectrum exists to estimate mel-

anoma-effective doses. Based on the reported relationship between sunburn and melanoma (11), we chose the Commission Internationale de l'Éclairage (CIE) erythema (sunburn) action spectrum (8) as a surrogate. This action spectrum is widely used as a standard, e.g., in calculations of the UV index (12), a globally accepted index that is a measure of biologically effective sunburning doses from sunlight for human skin.

For each source used in these experiments, the erythemally effective irradiance was calculated by measuring the spectral output (Fig. 1) and multiplying it by the CIE action spectrum for erythema as described above. The erythemally effective irradiance was used to calculate the erythemally effective or standard erythemal dose (SED). By convention, one SED is equivalent to 100 J/m² of erythemally weighted UV. For these studies, we chose a dose of 23 SED, determined previously to be melanomagenic in this mouse model (4). To illustrate the biological relevance of this dose, we made use of ground-based spectroradiometric measurements of sunlight from the United States National Science Foundation's UV monitoring network (13). At San Diego (32.7°N, 117.2°W), 23 SED were received in approximately 2 hours 40 minutes during noon-time on July 4, 2000.

The erythemally effective dose delivered to neonatal HGF/SF-transgenic mice from each of three UVB-containing sources was calculated to be 23 SED. These sources were the F40 sunlamp (250–800 nm), the solar simulator (290–800 nm), and the isolated UVB waveband (>96% 280–320 nm). For UVA exposure, it was necessary to use an absolute rather than a biologically effective dose because, as illustrated by the CIE action spectrum, UVA is much less effective than UVB in producing erythema.⁴ Under the environmental conditions described, >92% of the erythemally effective irradiance is delivered by UVB whereas <8% is accounted for by UVA. Exposure from the isolated UVA waveband (>99.9% 320–400 nm) was 150 kJ/m². This dose of UVA would have been received in approximately 50 minutes of sunlight exposure. In that time, an erythemal dose of about 7 SED would have been delivered, a dose determined to be melanomagenic (see below).

To establish if exposure pattern affected melanoma development, we first delivered the same absolute radiation dose from F40 sunlamps as a single treatment (14.7 kJ/m²; 23 SED) at 3 days of age as described previously (4). In a separate experiment, 14.7 kJ/m² was delivered as three equally fractionated treatments on days 3, 4, and 5 of age (Table 1). The same proportion of animals developed melanoma with similar median times of tumor appearance (Table 2). Kaplan-Meier survival analysis indicated no significant difference between the two groups ($P = 0.85$; data not shown), and data from these two groups were pooled for subsequent analysis. The number of treatments used for animals treated with each source is indicated in Table 1.

We next tested an earlier observation, derived using a melanoma model in the *Xiphophorus* fish, that UVA radiation can initiate melanoma (14), using two strategies. First, we determined the consequences of removing UVB from F40 sunlamps as follows: we compared the effects of neonatal exposure to equivalent absolute doses of radiation delivered from unfiltered F40 sunlamps, which emit UVB, UVA, and visible radiation, to the effects of the same lamps filtered with Mylar that removed 96.8% of the UVB (14.7 to 14.1 kJ/m², respectively; Fig. 1A; Table 1). Removal of UVB resulted in no junctional melanoma formation. One deep dermal melanoma similar to the unirradiated control group was observed (Fig. 2A; Table 2).

To verify and extend these observations, a second strategy was used. We undertook an evaluation of the effects of UV radiation in the mouse melanoma model, using either isolated wavebands of UVB or

⁴ Figs. 2 and 3 in http://www.cpc.ncep.noaa.gov/products/stratosphere/uv_index/uv_nature.html.

Table 1 UV sources and doses delivered to initiate melanoma in HGF/SF-transgenic mice

Source	Total radiation UV-vis (250–800 nm) kJ/m ²	Total UV A, B, & C (250–400 nm) kJ/m ²	Total UVA (320–400 nm) kJ/m ²	Total UVB (280–320) nm kJ/m ²	Peak UVB Wavelength (nm)	SED †	Number of treatments to deliver total dose
UVB filter with xenon arc	14.0	14.0	0.5	13.5	306	23	3
Unfiltered F40 sunlamp							
Single dose	14.7	9.5	3.3	6.2	313	23	1
Fractionated dose	14.7	9.5	3.3	6.2	313	23	3
Solar simulator:	322.1	41.9	36.0	5.9	320	23	1
Mylar filtered F40 sunlamp	14.1	4.0	3.8	0.2		0.1	1
UVA filter with xenon Arc	150.0	150.0	150.0	1.5e ⁻⁵		1.1	3
Nil	0	0	0	0		0	0

NOTE. For spectral output of sources, see Figure 1. Neonatal HGF/SF-transgenic mice and an equivalent number of wild-type littermates were irradiated at 3 to 5 days of age. † Standard erythemal doses calculated as described in the text.

Table 2 Melanomagenesis in UV irradiated HGF/SF-transgenic mice

Source	No. HGF/SF-transgenics	No. with melanoma	Median time to first melanoma (days)	Total no. of melanomas	Mean no. melanomas/tumor bearer	No. with metastatic melanoma
UVB filter with xenon arc	18	10	127	17	1.7	2
Unfiltered F40 sunlamp						
Single dose	23	6	169	6	1	1
Fractionated doses	19	5	174	5	1	1
Combined F40 sunlamp	42	11	174	11	1.0	2
Solar simulator	29	5	284	6	1.2	0
Mylar filtered F40 sunlamp	20	1		1	1	0
UVA filter with xenon arc	23	0		0	0	0
Nil	15	1		1	1	0

UVA or solar simulating radiation (Fig. 1B and C). A comparison of melanoma formation for these experimental groups indicated that only UVB-containing sources initiated melanoma. These were the unfiltered F40 sunlamp (250–800 nm), the isolated UVB waveband (>96% 280–320 nm), and the solar simulator (290–800 nm; Fig. 2A; Table 2). In contrast, animals irradiated with the isolated UVA waveband (>99.9% 320–400 nm) did not produce any melanomas. Comparison of the data for all three melanoma-effective sources indicated a significant positive trend for exposure to UVB ($P < 0.01$), a negative but not significant trend for exposure to UVA ($P = 0.07$) and no significant trend ($P = 0.10$) for total radiation (Tables 1 and 2; Fig. 2A and B). Underscoring this observation is data from a pilot study (data not shown) in which HGF/SF-transgenic animals were irradiated with a lower dose (4.5 kJ/m² absolute dose; 7 SED) of the isolated UVB waveband. This dose was very effective, producing a total of 10 melanomas in five animals from a cohort of 10 treated mice.

In contrast to the conclusions from the study of *Xiphophorus* fish as a model system for melanoma, in which UVA was reported to have melanoma-inducing properties (14), our data indicate that UVA (320–400 nm; Fig. 2A; Table 2) was not melanomagenic. In our study, UVA was ineffective as a melanomagenic agent even at a dose 33-fold greater than the highly potent lower dose (7 SED) of isolated UVB (150 kJ/m² versus 4.5 kJ/m²). In comparison, UVA/UVB ratios calculated with a radiation-transfer model to estimate sunlight exposure for typical mid-latitude summer conditions (solar zenith angle = 30°, total ozone column 250–450 Dobson units) under clear skies range approximately between 16 and 24.⁵ Thus, within the constraints of these comparisons and this model, there is a clear implication that in natural sunlight, UVB and not UVA, is the carcinogen for melanoma.

This finding has major implications for mechanism because UVB initiates DNA damage (15), signaling pathways (16, 17), and immune alterations (6, 18, 19) differently from UVA.

Additional analyses of these data further revealed a significantly greater efficiency in melanomagenesis for the isolated UVB waveband when compared to the F40 source or when compared to the solar simulator (tumor-free survival: modified log-rank test, $P < 0.02$; Fig. 2A and B). Melanomas were also initiated by the isolated UVB

waveband with a significantly lower median time to tumor ($P = 0.04$, Kruskal-Wallis; Table 2) than with the other two sources. The absolute dose of UVB (Table 1) delivered from the isolated UVB waveband (13.5 kJ/m²) was substantially higher than from the F40 sunlamp (6.2 kJ/m²) or from the solar simulator (5.9 kJ/m²), consistent with its greater effectiveness and suggesting a dose-response for melanoma formation. There was no significant difference between the F40 sunlamp and the solar simulator in median time to tumor ($P = 0.16$, Mann-Whitney) or in tumor-free survival (modified log-rank test, $P = 0.38$) consistent with the comparable absolute doses delivered. Because both the F40 source and the solar simulator contain a substantial proportion of UVA and visible radiation not found in the isolated UVB waveband (Table 1), it could be postulated that these wavelengths inhibited melanoma formation. However, we do not currently favor this interpretation because we found no significant difference in tumor-free survival between animals treated with the F40 sunlamp, which had a UVA/UVB ratio of 0.5:1, or with the solar simulator, which had a UVA/UVB ratio of 6:1 and delivered an 11 times higher UVA dose (3.3 kJ/m² versus 36.0 kJ/m², respectively).

Despite the fact that the absolute doses of UVB were consistent with the experimental observations, comparison of absolute doses of UV from the three melanoma-effective optical sources is not a robust evaluation of melanoma-inducing effectiveness. This is because the differential in wavelength effectiveness for a given photobiological effect is compounded by the differing wavelength outputs associated with each optical source. To account for this in this study, given the absence of a mammalian melanoma action spectrum, we used the standardized CIE erythemal action spectrum as described above to determine and then deliver identical erythemally effective doses (23 SED) from each of the three sources. Critically important was the observation that the survival data for all three groups were not superimposable as would be expected if the erythemally effective dose were an accurate measure of melanoma induction (Fig. 2A and B). In light of this observation, the CIE erythemal action spectrum, although valuable in estimating effective human sunburning doses, may not be an appropriate weighting function for evaluating melanoma-effective doses. These findings highlight a crucial need for experimental derivation of a mammalian action spectrum specifically for melanoma induction by UV. Other advantages of a melanoma action

⁵ G. Bernhard, personal communication; <http://www.libradtran.org/>.

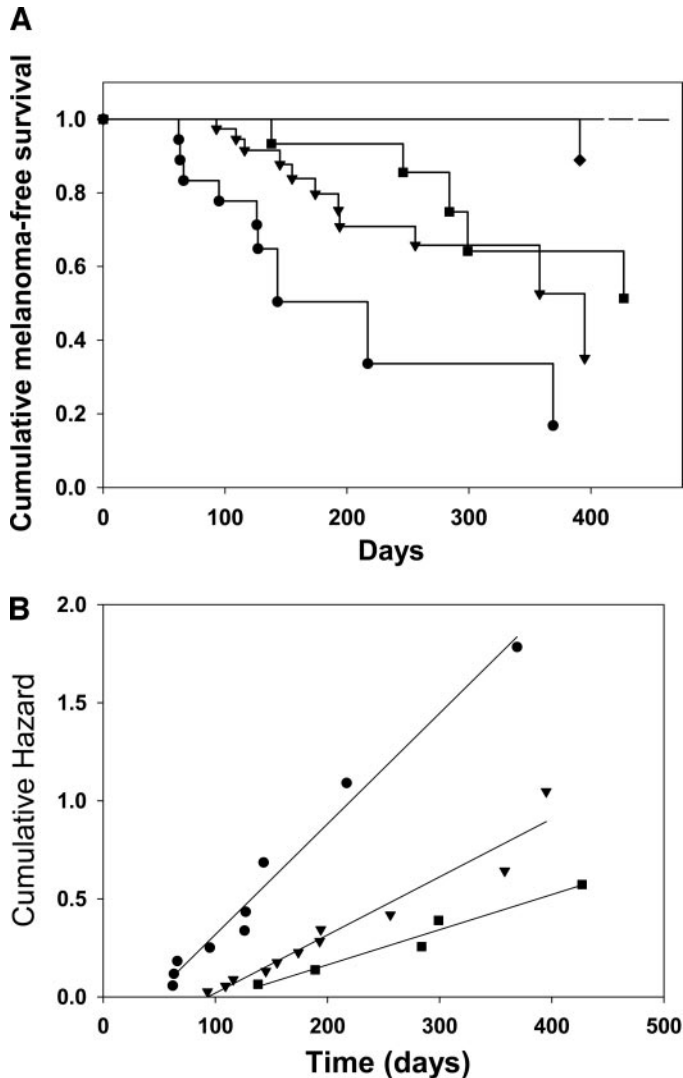


Fig. 2. Melanoma induction in neonatally UV-irradiated HGF/SF-transgenic mice. A, melanoma-free survival for animals treated with five radiation sources. For doses delivered, see Table 1, and for spectral outputs of each source, see Fig. 1. For the isolated UVB waveband (●), F40 sunlamp (▼) sources, and solar simulator (■), the dose delivered corresponded to 23 SED (see text). Melanoma-free survival for animals treated with F40 sunlamps with UVB removed by Mylar (◆) was significantly different from that for animals treated with the isolated UVB waveband, the F40 sunlamp, or the solar simulator (modified log-rank test, $P < 0.01$). Pairwise comparisons of melanoma-free survival by modified log-rank tests: UVB versus F40, $P < 0.02$; UVB versus Solar simulator, $P < 0.01$; Solar simulator versus F40, $P = 0.38$. Animals treated with the isolated UVA waveband produced no melanomas (dashed line). B, cumulative hazard (negative \ln cumulative survival from Fig. 2A) data points for the three melanoma-effective sources were fitted to a linear regression for each data set. All groups were irradiated with a total erythemally weighted dose of 23 SED. For all data sets $r^2 > 0.94$. The observed linearity suggests an exponential model and that the relative hazards are proportional. The relative hazard estimate based on survival without melanoma was significantly different for isolated UVB waveband (●) versus F40 (▼; $\chi^2 = 4.73$, $P = 0.03$) and for isolated UVB versus solar simulator (■, $\chi^2 = 7.65$, $P < 0.01$) but not significantly different for solar simulator versus F40 ($\chi^2 = 0.75$; $P = 0.39$). Comparison of the data for all three sources indicated a significant positive trend for exposure to UVB ($\chi^2 = 8.98$, $P < 0.01$), a negative but not significant trend for exposure to UVA ($\chi^2 = 3.3$, $P = 0.07$) and no significant trend for total radiation ($\chi^2 = 2.77$, $P = 0.10$).

spectrum would be its use as a weighting function for accurate estimation of melanoma-effective doses from different UV sources such as sunlight or artificial sources (20), its use in providing valuable information on the *in vivo* absorption spectrum of the principal target molecule involved in the UV initiation of melanoma aiding in its identification (1), and its use in suggesting molecular/genetic pathways for future study. These data would provide significant insight into an overall evaluation of the role of UV in melanoma risk.

Decades-long increases in melanoma incidence continue (21). Significant stratospheric ozone losses continue over polar regions as well as over populated areas (22). Notwithstanding the success of the Montreal Protocol in limiting global production and emission of ozone-destroying gases, a specific time frame for recovery of the stratospheric ozone layer, and mitigation of the associated increases in UVB remain highly uncertain (23, 24). Thus, given the direct connection between stratospheric ozone loss and increased UVB, an uncertain period of sustained UVB increases with potential impact on human health is anticipated.

Using the optical sources described, in conjunction with a unique experimental mouse melanoma model that closely recapitulates human disease, we have shown that discrete waveband analyses are possible for experimental melanoma induction. Significantly, we provide compelling evidence from the HGF/SF-transgenic mouse model that UVB radiation, but not UVA, initiates mammalian melanoma, suggesting that this disease belongs within the category of UVB effects. The close similarity of the melanomas formed in these experiments to human melanoma points to an important human relevance. Additionally, we show that erythemally effective doses of UV from artificial sources and, by extrapolation, from sunlight do not accurately estimate melanoma risk. For a correct assessment of risk involving UV radiation and melanoma, a melanoma action spectrum is needed. In future studies, we anticipate that by establishing the melanomagenic effectiveness of precisely defined narrower bands of radiation (6) within the UVB region, identification of the UV pathways relevant to melanoma will become possible. We conclude that our data not only provide a focus for future basic research in melanomagenesis, but also clearly indicate that for protection of melanoma-sensitive populations, minimizing exposure to UVB radiation is to be strongly recommended.

Acknowledgments

The authors gratefully acknowledge Dr. M. Anver and colleagues for histopathology and Drs. G. Bernhard, M. Repacholi, B. Bouscarel and N. Perrotti for manuscript review.

References

- Diffey BL. Solar ultraviolet radiation effects on biological systems. *Physics Med Biol* 1991;36:299–328.
- Recio JA, Noonan FP, Takayama H, et al. Ink4a/arf deficiency promotes ultraviolet radiation-induced melanomagenesis. *Cancer Res* 2002;62:6724–30.
- Noonan FP, Dudek J, Merlino G, De Fabo EC. Animal models of melanoma: an HGF/SF transgenic mouse model may facilitate experimental access to UV initiating events. *Pigment Cell Res* 2003;16:16–25.
- Noonan FP, Recio JA, Takayama H, et al. Neonatal sunburn and melanoma in mice. *Nature (Lond)* 2001;413:271–2.
- Whiteman DC, Whiteman CA, Green AC. Childhood sun exposure as a risk factor for melanoma: a systematic review of epidemiologic studies. *Cancer Causes Control* 2001;12:69–82.
- De Fabo EC, Noonan FP. Mechanism of immune suppression by ultraviolet irradiation in vivo. I. Evidence for the existence of a unique photoreceptor in skin and its role in photoimmunology. *J Exp Med* 1983;158:84–98.
- Webber LJ, Whang E, De Fabo EC. The effects of UVA-I (340–400 nm), UVA-II (320–340 nm) and UVA-I+II on the photoisomerization of urocanic acid in vivo. *Photochem Photobiol* 1997;66:484–92.
- McKinlay AF, Diffey BL. A reference action spectrum for ultraviolet-induced erythema in human skin. In: Passchier WF, Bosnjakovic BF, editors. Human exposure to ultraviolet radiation; risk and regulations. Amsterdam: Elsevier; 1987. p. 83–7.
- Young AR, Chadwick CA, Harrison GI, et al. The similarity of action spectra for thymine dimers in human epidermis and erythema suggests that DNA is the chromophore for erythema. *J Invest Dermatol* 1998;111:982–8.
- Noonan FP, De Fabo EC. Relationships between changes in solar UV spectra and immunologic responses. In: Young A, Björn LO, Moan J, and Nultsch W editors. *Environmental Photobiology*. New York: Plenum Press; 1993. p. 113–48.
- Veierod MB, Weiderpass E, Thorn M, et al. A prospective study of pigmentation, sun exposure, and risk of cutaneous malignant melanoma in women. *J Natl Cancer Inst (Bethesda)* 2003;95:1530–8.
- World Meteorology Organization (WMO). Report of the WMO-WHO meeting of experts on standardization of UV indices and their dissemination to the public, No.

127. Geneva, Switzerland: World Meteorological Organization. Global Atmospheric Watch Report; 1998.
13. Booth CR, Lucas TB, Morrow JH, et al. The United States National Science Foundation's polar network for monitoring ultraviolet radiation. In: Weiler CS, Penhale PA editors. Ultraviolet radiation in Antarctica: measurements and biological effects. Washington DC: American Geophysical Union; 1994. p. 17-37.
14. Setlow RB, Grist E, Thompson K, Woodhead AD. Wavelengths effective in induction of malignant melanoma. *Proc Natl Acad Sci USA* 1993;90:6666-70.
15. Ravanat JL, Douki T, Cadet J. Direct and indirect effects of UV radiation on DNA and its components. *J Photochem Photobiol B* 2001;63:88-102.
16. Bode AM, Dong Z. Mitogen-activated protein kinase activation in UV-induced signal transduction. *Sci STKE* 2003;2003: RE2.
17. Bowden GT. Prevention of non-melanoma skin cancer by targeting ultraviolet-B-light signalling. *Nat Rev Cancer* 2004;4:23-35.
18. Reeve VE, Tyrrell RM. Heme oxygenase induction mediates the photoimmunoprotective activity of UVA radiation in the mouse. *Proc Natl Acad Sci USA* 1999;96:9317-21.
19. Garssen J, de Gruijl F, Mol D, et al. UVA exposure affects UVB and cis-urocanic acid-induced systemic suppression of immune responses in *Listeria monocytogenes*-infected Balb/c mice. *Photochem Photobiol* 2001;73:432-8.
20. Young AR. Tanning devices—fast track to skin cancer? *Pigment Cell Res* 2004;17: 2-9.
21. Ries L, Eisner M, Kosary C et al. SEER Cancer Statistics Review, 1975-2000. National Cancer Institute (Bethesda). 2003 [cited 23 April 04]. Available from: http://seer.cancer.gov/csr/1975_2000.
22. World Meteorology Organization (WMO). Scientific assessment of ozone depletion: 2002, Global ozone research and monitoring project - report no. 47. Geneva, Switzerland: World Meteorological Organization; 2003. p. 1-498.
23. Solomon S. The hole truth. What's news (and what's not) about the ozone hole. *Nature (Lond)* 2004;427:289-91.
24. Rex M, Salawitch RJ, von der Gathen P et al. Arctic ozone loss and climate change. *Geophys Res Lett* 2004;31:LO4116.